Myxoma virus infection of primary human fibroblasts varies with cellular age and is regulated by host interferon responses.

Johnston, J. B.; Nazarian, Steven H.; Natale, Renato; McFadden, Grant

Publisher's version / Version de l'éditeur:
https://doi.org/10.1016/j.virol.2004.11.030
Virology, 332, February 1, pp. 235-248, 2004-12-22

Available online at www.sciencedirect.com

SCIENCE DIRECT

Virology 332 (2005) 235–248

VIROLOGY

www.elsevier.com/locate/yviro

Myxoma virus infection of primary human fibroblasts varies with cellular age and is regulated by host interferon responses

J.B. Johnston[a,1], Steven H. Nazarian[a,b], Renato Natale[c], Grant McFadden[a,b,*]

[a]*BioTherapeutics Research Group, Robarts Research Institute, 1400 Western Road, London, ON, Canada N6G 2V4*
[b]*Department of Microbiology and Immunology, University of Western Ontario, London, ON, Canada N6G 2V4*
[c]*Department of Obstetrics and Gynaecology, SJHC/LHSC, 268 Grosvenor Avenue, London, ON, Canada N6G 4V2*

Received 22 September 2004; returned to author for revision 22 October 2004; accepted 9 November 2004
Available online 22 December 2004

Abstract

Recent studies have indicated a critical role for interferon (IFN)-mediated antiviral responses in the host range of myxoma virus (MV), a pathogenic poxvirus of rabbits. To investigate the contribution of IFN to MV tropism in nonleporine cells, primary human dermal fibroblasts (HDFs) were tested for permissiveness to MV infection. Low-passage HDFs that underwent fewer than 25 population doublings (PD) were fully permissive for MV infection, supporting productive virus replication and cell-to-cell spread. In contrast, early and late viral gene expression was detectable in high-passage HDF (>75 PD), but MV failed to generate infectious progeny and could not form foci in these cells. Vesicular stomatitis virus (VSV) plaque reduction assays confirmed that constitutive IFN production progressively increased as HDFs were passaged, concurrent with an increase in the expression of transcripts for type I IFN and IFN-responsive genes involved in antiviral responses. These findings correlated with the enhanced sensitivity of higher-passage HDF to inducers of type I IFN responses, such as dsRNA. Furthermore, pretreatment of low-passage HDF with type I IFN abrogated MV spread and replication while treatment of mature HDF with neutralizing antibodies to IFN-β, but not IFN-α, restored the capacity to form foci. These findings emphasize the importance of post-entry events in determining the permissiveness of human cells to MV infection and support a critical role for innate type I IFN responses as key determinants of poxvirus host range and species restriction.

Keywords: Poxvirus; Myxoma virus; Tropism; Host range; Interferon; Antiviral responses

Introduction

Myxoma virus (MV) is a leporipoxvirus that is the causative agent of myxomatosis, a lethal disease of European rabbits that presents with extensive fulminating lesions, immune dysfunction, and secondary bacterial infections of the respiratory tract (Fenner and Ratcliffe, 1965). Although MV exhibits strict species specificity for the rabbit and is nonpathogenic in other vertebrates, growing evidence indicates that MV can productively infect cells from diverse species in vitro. For example, MV has been recently shown to replicate in select murine cells (Johnston et al., 2003), as well as a broad spectrum of human tumor cell lines (Sypula et al., 2004). For most pathogens, the requirement for species-specific cell surface receptors that mediate virus entry is a critical determinant of host range (Mims, 1989; Schneider-Schaulies, 2000). However, no specific host cell receptor has ever been identified as being obligatory for infection by any poxvirus (Moss, 2001), suggesting that virus–host interactions that follow adsorption and entry of target cells determine permissiveness to poxvirus infection.

* Corresponding author. BioTherapeutics Research Group, Robarts Research Institute, Room 133 Seibens-Drake Building, 1400 Western Road, London, ON, Canada N6G 2V4. Fax: +1 519 663 3847.
E-mail addresses: james.johnston@nrc-cnrc.gc.ca (J.B. Johnston), snazarian@robarts.ca (S.H. Nazarian), renato.natale@sjhc.london.on.ca (R. Natale), mcfadden@robarts.ca (G. McFadden).
[1] Current address: Institute for Nutrisciences and Health, National Research Council of Canada, 93 Mount Edward Road, Charlottetown, PE, Canada C1A 5T1.

0042-6822/$ - see front matter © 2004 Elsevier Inc. All rights reserved.
doi:10.1016/j.virol.2004.11.030

MV has adapted to replicate successfully in the presence of vigorous host immunity by employing numerous strategies to evade, obstruct, or subvert elements that mediate antiviral responses to infection (Kerr and McFadden, 2002; Seet et al., 2003). In addition to sharing the ultimate goal of creating an intracellular environment that promotes productive virus infection, a central component of many of these strategies is the ability to manipulate cell signaling pathways critical to host antiviral responses (Greber, 2002). For example, MV infection rapidly activates kinase-mediated signal transduction that facilitates downstream events leading to productive infection (Johnston et al., 2003; Masters et al., 2001), inhibition of which renders cells nonpermissive (Johnston et al., 2003; Lalani et al., 1999). More recently, MV has also been shown to target signaling pathways involving nuclear factor (NF)-κB (Camus-Bouclainville et al., 2004). Although the actions of many of the immunomodulatory proteins encoded by MV are dispensable for replication in culture, they are often essential for replication within the host (Kerr and McFadden, 2002). Thus, the pathways targeted by MV to manipulate innate and adaptive host defense mechanisms have important consequences for viral tropism and the pathogenic effects of viral infections and may provide insight into the molecular mechanisms underlying poxvirus host range.

Recently, host antiviral responses mediated by type I interferon (IFN), which includes IFNα and IFNβ (Lau and Horvath, 2002), have been implicated as key determinants of the restrictive host range exhibited by MV in murine cells (Wang et al., 2004). Infected cells are likely capable of multiple response pathways to induce type I interferon-regulated genes, but it is believed that the virus–host tug-of-war is exerted in particular at the level of interferon regulatory factor (IRF)-3 activation, which is one of the key regulators of IFN-β gene expression (reviewed in Barnes et al., 2002; Levy et al., 2003; Malmgaard, 2004; Servant et al., 2002; Williams and Sen, 2003). If type I IFN is produced as a consequence of virus infection, the ligand is released into the extracellular milieu where it acts in both an autocrine and a paracrine fashion, binding to specific receptors on the surface of both infected and uninfected cells. This interaction activates signaling cascades, such as the signal transducer and activator of transcription (STAT)-janus kinase (JAK) pathway, leading to the expression of interferon-responsive genes. The activity of the resulting gene products promotes an antiviral state that decreases the susceptibility of uninfected cells to subsequent infection and impedes virus spread.

In fact, the actions of IFN are so effective at controlling the spread of viruses that all poxviruses employ at least one mechanism to disrupt their activity (Seet et al., 2003). These mechanisms primarily target host responses activated by dsRNA produced within infected cells during virus transcription, such as the IFN-dependent enzymatic cascades mediated by double-stranded RNA (dsRNA)-dependent protein kinase R (PKR) and the 2′,5′-oligoadenylate synthetase (OAS) (reviewed in Katze et al., 2002; Malmgaard, 2004; Taniguchi and Takaoka, 2002; Williams and Sen, 2003). PKR and OAS regulate response pathways that impede viral replication at multiple levels, promoting cell cycle arrest, a shutdown of host and virus protein synthesis and apoptosis. In an effort to inhibit these pathways, MV is predicted to encode a competitively inhibiting structural mimic of eukaryotic initiation factor (eIF)-2α, a substrate of PKR that induces growth arrest (Ramelot et al., 2002), as well as a dsRNA binding protein (Barrett et al., 2001). However, the exact mechanism of action for these proteins remains unclear.

In the current study, primary human dermal fibroblasts (HDFs) derived from neonatal foreskin explants were used to further investigate the contribution of type I IFN to MV host range and cell tropism. Neonatal HDFs initially exhibit decreased basal level IFN activity following explantation that increases with progressive population doublings (PD) as cells are passaged in vitro, a process commonly used as a model for cellular aging and the progression toward senescence (Komatsu et al., 1981; St. Geme and Horrigan, 1969). This progression manifests with increased type I IFN production, elevated levels of transcripts for IFN-responsive genes, and increased sensitivity to inducers of type I IFN responses. Of note, these properties are not unique to human fibroblasts, and similar responses have been reported for fibroblasts from other species, such as chick embryo fibroblasts (Lockart, 1968; Marcus and Carver, 1967) and murine L-cells (Jordan and Merigan, 1974).

Consistent with a critical role for IFN responses as determinants of MV host tropism, we report that primary HDFs are initially permissive to MV replication, but become refractory to MV infection with repeated passaging in culture. This loss of permissiveness correlates with increased basal levels of IFN activity in high-passage HDF compared to low-passage cells and can be completely reversed by inhibiting host IFN responses. These findings emphasize the importance of early events following recognition and entry of target cells in determining permissiveness to poxvirus infection and suggest a major role for IFN responses in the maintenance of the species barrier exhibited by many poxviruses.

Results

Human dermal explant cultures are permissive to MV infection

Primary HDFs were selected as a model system for these studies for several reasons. First, virus-enriched discharge from skin lesions that characterize MV infection of rabbits supports transmission of the virus by direct contact with an infected host, or more typically, via arthropod vectors such as the mosquito (Fenner and

Ratcliffe, 1965). Consequently, fibroblasts within the dermis are among the first cell types initially colonized by MV at the primary site of infection before it is disseminated to peripheral tissues. Second, transformed fibroblasts from several species, including human and nonhuman primate, murine, avian, and feline cells, have been found to support MV replication in vitro (Comanita and Dekaban, 2004; Johnston et al., 2003; Lalani et al., 1999; Sypula et al., 2004). Finally, changes in host IFN responses following aging in culture have been well documented for primary fibroblasts (Jordan and Merigan, 1974; St. Geme and Horrigan, 1969). Thus, the effects on MV replication of changes in constitutive IFN activity and responsiveness could be assessed in a naturally developing system using cells derived from the same donor.

The block to MV replication in nonpermissive cells most commonly manifests as the failure to progress through viral DNA synthesis to the late gene expression necessary to produce progeny virions, despite normal virus binding, entry, and early gene expression (Johnston et al., 2003). To determine if MV could infect primary human dermal cells, explants from neonatal foreskin tissue were prepared and allowed to adhere to culture dishes to stimulate cell outgrowth. Proliferating cells, initially classified as either fibroblast (HDF) or epithelial cells (HEP) on the basis of morphology, were typically observed after 5 days in culture and formed intact cell monolayers by 21 days (Figs. 1A and E). Outgrowth cultures were then infected at an multiplicity of infection (MOI) = 1 with either vMyxgfp (Figs. 1B–F) or vMyxlac (Figs. 1G and H) and viral replication was assessed at various time points PI by fluorescence microscopy or β-galactosidase assay, respectively. Green fluorescent protein (GFP) fluorescence was detected in both the explant and individual cells within HDF monolayers at 16 h PI (Fig. 1B), suggesting that these cells supported virus entry and early gene expression. Moreover, MV exhibited the capacity to spread and replicate within the monolayer, giving rise to large foci at 40 h (Fig. 1C) and 60 h (Fig. 1D) PI. Early gene expression was also evident in HEP cultures infected with vMyxgfp (Fig. 1F), although less viral spread was observed compared to HDF. Detection of β-galactosidase activity and foci formation at 40 h (Fig. 1E) and 60 h (Fig. 1F) following infection of HDF with vMyxlac further supported the capacity for MV to replicate and spread within these cells. To confirm that the GFP and β-galactosidase expression detected in MV-infected HDF was evidence of viral protein synthesis, the expression of representative early and late MV proteins was assessed by Western blot analyses at 6 and 16 h PI. Expression of both the early protein M-T7 (Fig. 1I), and the late protein Serp-1 (Fig. 1J) was detected in HDF and HEP following MV infection. These findings demonstrated that there was no block to MV entry, early or late gene expression, or DNA synthesis in primary human dermal cells. Moreover, similar results were obtained using HDF obtained from multiple donors.

Primary HDFs are permissive to MV replication

The foci formation observed in MV-infected human dermal cell cultures suggested that progeny virions were both being produced and spreading to adjacent cells within the monolayer. To determine if these cells were in fact permissive to MV replication, rapidly replicating HDFs were isolated from slowly replicating HEP cells and the purity of each cell population confirmed by RT-PCR detection of fibroblast-specific markers (data not shown). Single-step growth curves (Fig. 2A), for which cells were infected at high MOI to provide insight into MV replication at the single-cell level, and multistep growth curves (Fig. 2B), for which cells were infected at low MOI to assess replication and spread within a population of cells, were then generated for each cell type. As shown in Fig. 2, primary HDFs were fully permissive to MV infection and supported the production of progeny virions following infection at both high and low MOI. Moreover, single-step growth curves indicated that HDF supported MV replication at levels comparable to primary rabbit dermal fibroblasts (RDF) (Fig. 2A). In contrast, despite the ability to detect both early and late viral gene expression, MV was unable to generate progeny virus in HEP cells regardless of MOI. For both single- and multistep curves, the viral titers obtained from HEP cells did not significantly exceed the input titer of the original inoculum. These findings represent the first report of the productive infection of a primary human cell line by MV and indicate that this capacity is cell type dependent. In addition, these findings indicated that there was no fundamental block to MV replication in primary HDF once viral entry had occurred, provided that the IFN response is not engaged.

High-passage HDFs fail to support MV replication

Since HEP cells did not support productive MV replication, subsequent experiments focused on MV infection of primary HDF. However, attempts to investigate the molecular mechanism underlying the permissiveness of HDF to MV infection revealed an interesting and reproducible trend. As shown in Figs. 3A and B, HDFs that were passaged fewer than five times, corresponding to approximately 25 population doublings (PD), remained fully permissive to MV infection. As with the explant cultures from which these cells were derived, MV infection of low-passage HDF resulted in abundant β-galactosidase activity (Fig. 3E) and led to the production of infectious progeny virions (Fig. 3F). In contrast, cells that were repeatedly passaged (Figs. 3C and D) gradually became progressively resistant to MV infection until foci formation was no longer detectable after passage 10 (approximately 50 PD). Loss of foci formation was accompanied by decreased β-galactosidase activity (Fig. 3E) and the inability to support a productive infection (Fig. 3F). In comparison, little difference in viral titers and β-galactosidase activity was

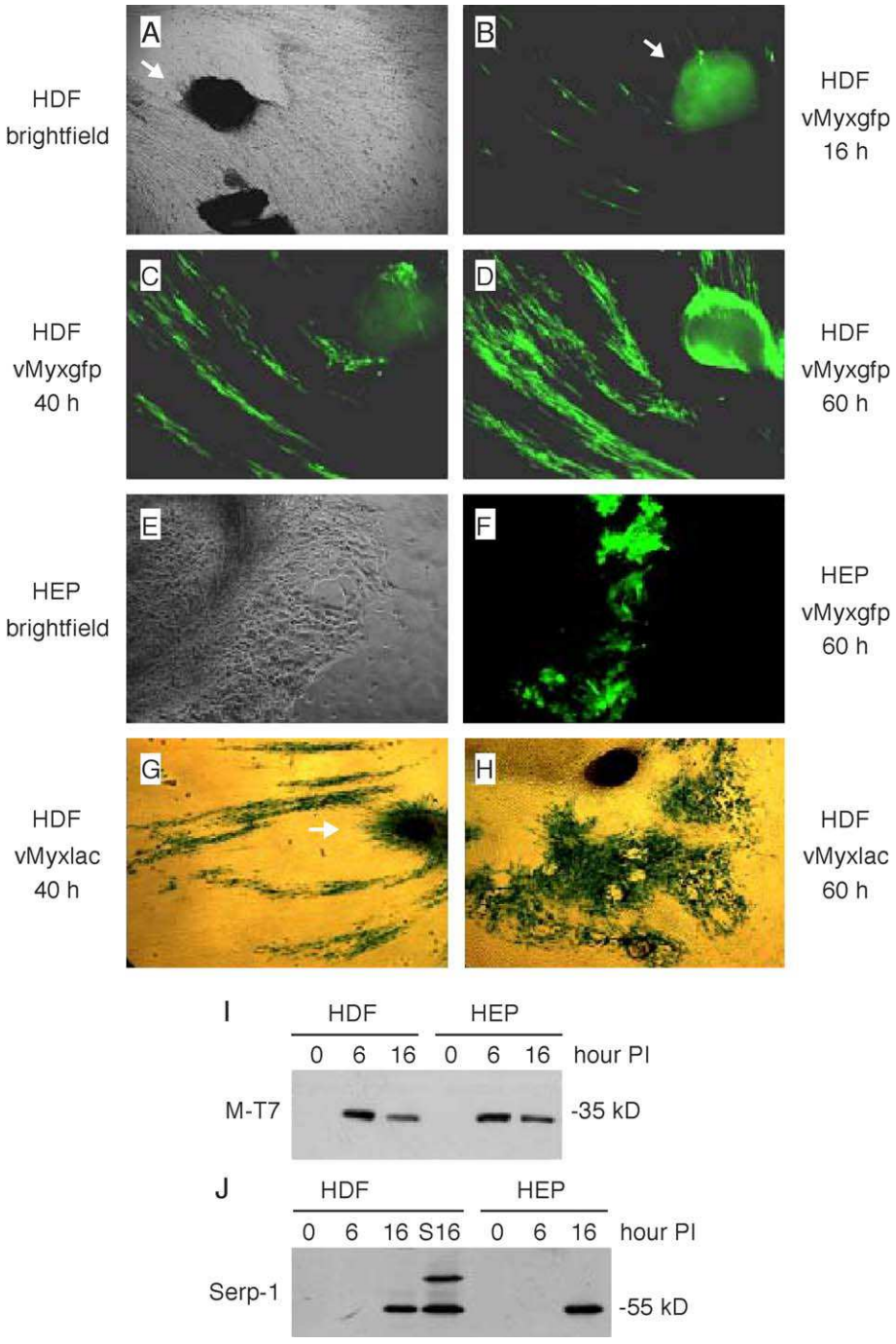

Fig. 1. MV infection of primary HDF. Three-week-old HDF and HEP explant cultures were infected with MV at MOI = 1 and assessed for viral replication and viral gene expression at various times PI. The explants from which cells originated are indicated by an arrow. (A–D) Fluorescence microscopy detection of HDF infected with vMyxgfp at 16 h (B), 40 h (C), and 60 h (D) PI. A representative brightfield micrograph is shown (A). (E and F) Brightfield (E) and fluorescence (F) microscopy detection of HEP infected with vMyxgfp. (G and H) β-Galactosidase staining of vMyxlac-infected HDF at 40 h (G) and 60 h (H) PI. (I and J) Western blot detection of the expression of representative early (M-T7) and late (Serp-1) MV genes. Detection of secreted Serp-1 in culture supernatants from HDF collected at 16 h PI is shown (S16).

observed when P1 and P5 RDF cultures were compared (Figs. 3E and F). Early gene expression was still detectable in both high- and low-passage HDF by fluorescence microscopy following infection with vMyxgfp (Figs. 3A–D, insets) and by Western blot detection of M-T7 expression (Fig. 3G). However, GFP expression was decreased in high-passage HDF and the late MV protein Serp-1 was not immediately observed in lysates from P5 and P10 cultures (Fig. 3G). Since β-galactosidase activity was still evident in the sporadic foci evident in P5 HDF (Fig. 3C) and as individual positive cells in P10 cultures (Fig. 3D), it is likely that Serp-1 levels were sufficiently

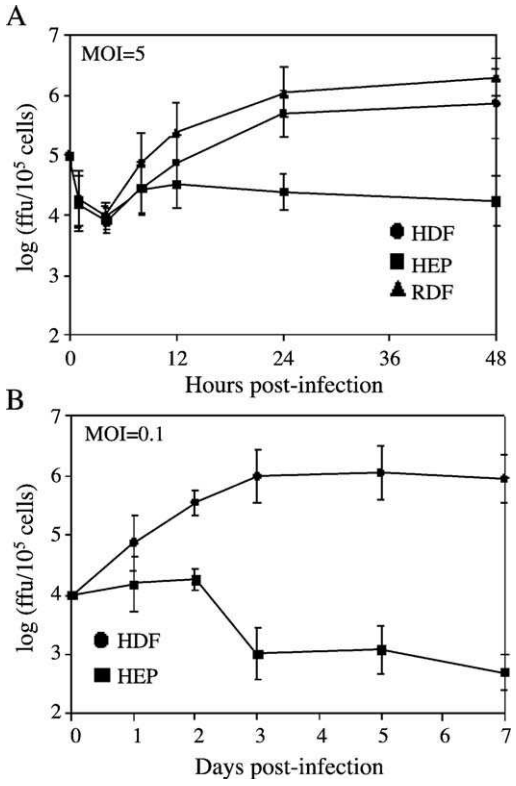

Fig. 2. MV infection of primary HDF is productive. HDF, HEP, and RDF were infected with vMyxlac and viral replication assessed by titration of infectious progeny on BGMK cells. Titers at each time point represent the mean focus forming units ± standard deviation (SD) from triplicate wells. (A) Single-step growth curve derived from low-passage cells infected at MOI = 5. (B) Multistep growth curve derived from low passage cells infected at MOI = 0.1

reduced so as to be undetectable by Western blot analysis. Consistent with this hypothesis, and similar to MV-infected HEP cells, overexposure of the blots shown in Fig. 3H did reveal low-level Serp-1 expression (data not shown). These findings suggest that repeated passage of primary HDF in vitro promoted the development of an antiviral state refractory to sustained MV replication. Moreover, the block to MV replication did not simply represent failure to progress to late MV gene expression but appeared to reflect a decreased capacity to spread within the monolayer and form foci.

High-passage HDFs exhibit enhanced sensitivity to dsRNA

In an effort to determine the mechanism underlying the loss of permissiveness associated with sustained passage, we first addressed the question of whether MV infection of high-passage HDF was cytotoxic. For these studies, P1 and P10 HDFs were infected with MV at different MOI and cell viability was assessed by trypan blue exclusion assay at 12 h PI. Although minimal differences were observed between low- and high-passage HDF infected at MOI = 0.1, cell death was significantly increased in P10 cells infected at MOI = 5 compared to P1 HDF (Fig. 4A). A similar pattern was observed when parallel HDF cultures were analyzed by flow cytometry following staining with Annexin V to detect cells actively undergoing apoptosis. Infection of P10 HDF with MV at high multiplicities induced an apoptotic response that was not evident in MV-infected P1 HDF cultures (Fig. 4B). Again, no differences were observed when cells were infected at MOI = 0.1 (Fig. 4B).

To further dissect this process, we next tested the sensitivity of high- and low-passage HDF to various stress stimuli associated with cell cycle arrest. As with low multiplicity infections, similar levels of cell death and apoptosis were detected in both high- and low-passage HDFs subjected to serum deprivation and treatment with pro-apoptotic drugs that inhibit proteasome (LLnL) or protein kinase C (staurosporine, STS) activity (Figs. 4A and B). However, high-passage HDFs were approximately 2.5-fold more sensitive than low-passage cells to the cytotoxic effects of poly(I:C) dsRNA, a by-product of viral transcription that induces host IFN responses in infected cells (Tamura and Sasakawa, 1983). Taken together, these findings indicated that the loss of permissiveness exhibited by high-passage HDF could be attributed, at least in part, to accelerated cell death following MV infection. Moreover, this property was associated with increased sensitivity to the inhibitory effects of dsRNA.

The IFN response pathway is constitutively activated in high-passage HDF

The observation that high-passage HDFs were more sensitive than low-passage cells to dsRNA implicated host IFN responses as potential determinant of the loss of permissiveness exhibited by primary HDF following passaging. This hypothesis was further supported by the finding that individual high-passage HDFs were permissive to MV infection, although the infection was abortive due to a cytotoxic response, but that MV was unable to spread to adjacent cells within the monolayer (Fig. 3). As detailed above, Type I IFN acts to limit infections by promoting both clearance of infected cells and the development of an antiviral state in uninfected cells that impedes virus spread.

To determine at which level IFN responses were altered, HDFs of varying passage histories were cultured for 24 h and protein, RNA, and conditioned medium (CM) harvested for subsequent analysis. RT-PCR detection of IFN-β transcripts revealed that constitutive IFN expression increased as HDFs were passaged, such that IFN-β was not detectable in low-passage HDF but was abundantly expressed in P10 cells at levels comparable to that found in P1 HDF stimulated with dsRNA (Fig. 5A). Moreover, the expression of elements within the IFN response pathway, such as PKR and OAS, exhibited a similar profile. PKR and OAS were constitutively expressed at higher levels in P10 HDF than P1 HDF (Fig. 5A). Western blot analyses of other elements within the IFN response pathway, such as PKR and its

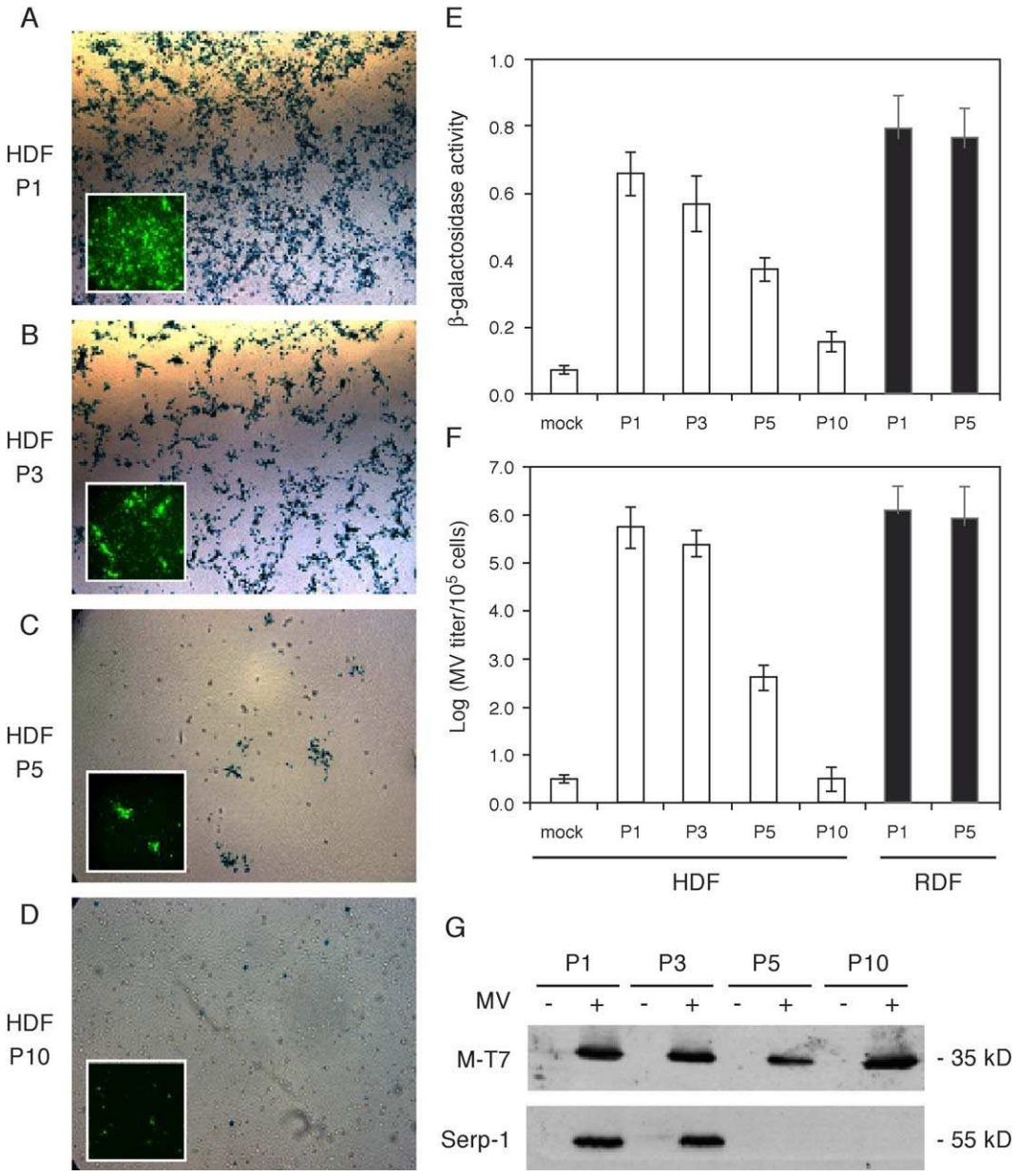

Fig. 3. Loss of permissiveness to MV infection with repeated passaging of HDF. HDF (clone A9) and RDF (clone A1) were cultured for the indicated number of passages (one passage represents five population doublings) prior to being infected with vMyxlacZ at MOI = 1. (A–D) HDF cultures were passaged 1 (A, P1), 3 (B, P3), 5 (C, P5), or 10 (D, P10) times and infected with vMyxlac at MOI = 1. Foci were detected by β-galactosidase staining at 48 h PI. Parallel HDF cultures were infected with vMyxgfp (insets) and early viral gene expression visualized by fluorescence microscopy. (E) Quantification of the level of β-galactosidase expression at 48 h PI of HDF and RDF cultures. Values represent mean absorbance ± SD (corrected for background) from triplicate wells with mock-infected cells as a control. (F) Viral titers obtained at 48 h PI of HDF and RDF. Values represent mean focus forming units ± SD from triplicate wells. (G) Western blot detection of early (M-T7) and late (Serp-1) MV gene expression following vMyxlac infection of passaged HDF.

cellular target eIF-2α, and the transcription factor STAT-1, yielded similar results. As suggested by RT-PCR, PKR was detectable by Western blot in virtually all HDF cultures regardless of passage history (Fig. 5B). Activated PKR phosphorylated on Thr457, however, was only detected in high-passage HDF in the absence of exogenous stimuli. Recent evidence has shown that PKR can be activated independent of dsRNA by cellular regulators, such as PACT, which interact with the enzyme through its dsRNA-binding motifs and enhance phosphorylation of eIF-2α (Patel and Sen, 1998). The stimuli for this activation include a variety of stress signals similar to those induced by sustained passage of HDF (Patel et al., 2000). Consistent with the finding that PKR is constitutively activated in high-passage HDF, phosphorylation of eIF-2α on Ser51, the residue targeted by activated PKR, was evident only in P10 HDF despite the ability to detect eIF-2α protein in most cultures (Fig. 5B). It should be noted that infection with MV or treatment with dsRNA further increased phosphorylation of PKR above the elevated basal level detectable in high-

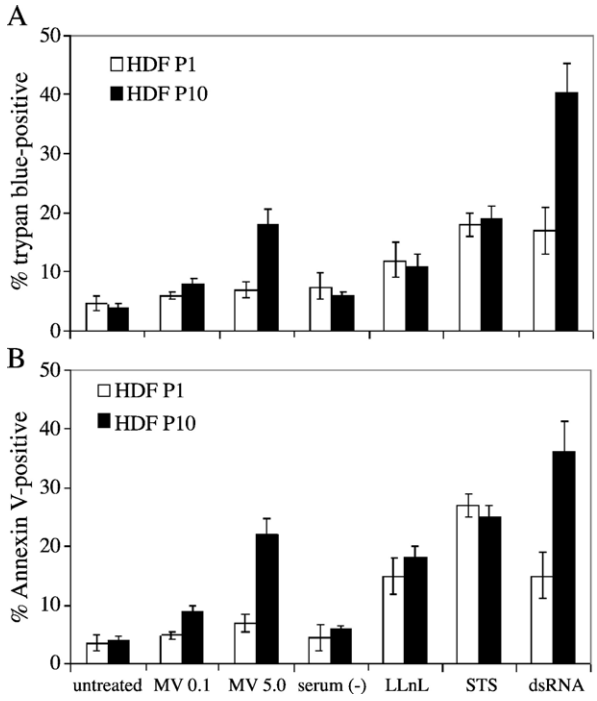

Fig. 4. High-passage HDFs exhibit increased sensitivity to dsRNA. Low (P1)- and high (P10)-passage HDFs were subjected to various stress stimuli and cell viability assessed at 12 h posttreatment by trypan blue exclusion (A) or FACS detection of Annexin V staining (B). Stimuli included infection with vMyxlac at MOI = 0.1 or 5, serum deprivation, and treatment with LLnL (10 nM), staurosporine (STS, 50 nM), or poly(I:C) dsRNA (20 μg/ml). Untreated cells served as a control. (A) Values represent the mean number of trypan blue-positive cells ± SD from triplicate wells as a percentage of total cells. (B) Values represent the mean number of Annexin V-positive/PI-negative cells ± SD from duplicate samples that were.

passage HDF (data not shown), indicating that like low-passage HDF these cells remained responsive to external stimuli known to activate IFN responses.

Although STAT-1 protein levels did not vary significantly with passage history, STAT-1 phosphorylated on either Tyr701 or Ser727 was detected in high-passage HDF but not in low-passage cells (Fig. 5B). Since phosphorylation is a prerequisite for the activation of STAT-1 and its subsequent translocation to the nucleus where it promotes transcription of IFN-responsive genes, this finding suggested that STAT-1 was also constitutively activated in high-passage HDF. Immunofluorescence staining of STAT-1 in high- and low-passage HDF confirmed this result. STAT-1 was detected primarily in the cytosol of P1 HDF, but was abundant in the nucleus of P10 HDF in the absence of exogenous stimuli where it colocalized with the nuclear satin, DAPI (Fig. 5C).

Previous findings suggested that elements within the IFN response pathway were constitutively upregulated and activated in HDF as a result of sustained passage in vitro. To determine whether these results correlated with increased IFN production and biological activity, vesicular stomatitis virus (VSV) plaque reduction assays were conducted using CM from passaged HDF. VSV infection is extremely sensitive to the inhibitory effects of Type I IFN and inhibition VSV replication remains the gold standard by which IFN activity is determined (Julkunen et al., 1982). Compared to untreated cells infected with VSV, pretreatment with human IFN-β (5 U/ml) completely blocked VSV replication and inhibited plaque formation in BHK cells (Fig. 5D). Preincubation of BHK cells with CM from P1 and P3 HDF cultures had little impact on VSV plaque formation, suggesting that little or no biologically active IFN was being constitutively produced by these cells (Fig. 5D). In contrast, CM from high-passage HDF significantly inhibited VSV replication, reducing plaque formation by approximately 50% when CM from P10 HDF was used (Fig. 5D). This effect was attributable to the activity of IFN since CM pretreated with neutralizing antibodies to IFN-β, but not IFN-α, failed to inhibit VSV replication (Fig. 5D).

These results suggest that repeated passage of HDF upregulated IFN expression and resulted in constitutive activation of the IFN response pathway and increased sensitivity to stimuli that induce IFN responses, such as dsRNA. However, it should be noted that low-passage HDFs were not deficient in their ability to respond to stimuli known to induce an IFN response. Treatment of P1 HDF with poly(I:C) dsRNA induced or increased expression of IFN-β, OAS, and PKR transcripts (Fig. 5A), activated PKR, eIF-2α, and STAT-1α as determined by Western blot detection of the phosphorylated forms of these proteins (Fig. 5B) and promoted the production and release of IFN capable of inhibiting VSV replication (Fig. 5D).

IFN neutralization promotes MV replication in high-passage HDF

Given the potential link between the IFN and the capacity for passaged HDF to support MV replication, the effect of promoting or inhibiting IFN responses on MV replication was investigated in low (P1)- and high (P10)-passage cells. P1 HDF infected with vMyxlac in the presence of poly(I:C) dsRNA retained the ability to support foci formation (Fig. 6B) and productive infection (Fig. 6H). However, the intensity of β-galactosidase staining (Fig. 6G) and the magnitude of viral titers obtained (Fig. 6H) were decreased relative to untreated cells (Fig. 6A). The results of Fig. 5 demonstrated that the IFN response pathway was activated in low-passage HDF treated with dsRNA; thus, parallel experiments were conducted in which cells were pretreated with poly(I:C) dsRNA for 12 h prior to infection. Under these conditions, both foci formation and viral titers were significantly reduced (data not shown). In comparison, pretreatment of P1 HDF with IFN-β completely blocked foci formation (Fig. 6C) and abrogated viral replication (Fig. 6H). As observed in high-passage cells infected with MV, individual β-galactosidase-positive cells were evident in IFN-stimulated P1 cultures (Fig. 6C); thus, the block to MV replication was at the level of viral spread.

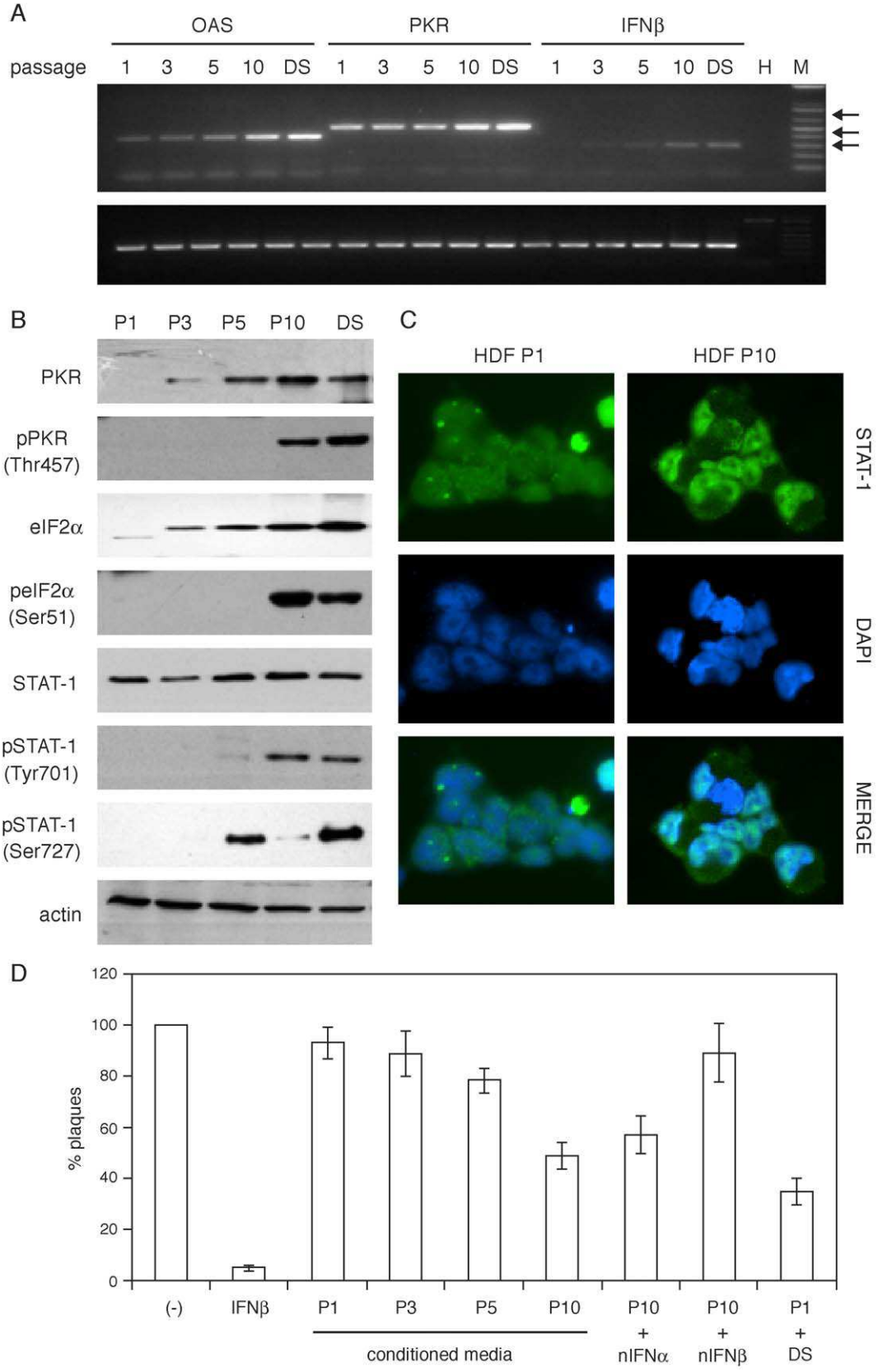
A
OAS
PKR
IFNβ
passage
1 3 5 10 DS 1 3 5 10 DS 1 3 5 10 DS H M
B
P1 P3 P5 P10 DS
PKR
pPKR (Thr457)
eIF2α
peIF2α (Ser51)
STAT-1
pSTAT-1 (Tyr701)
pSTAT-1 (Ser727)
actin
C
HDF P1
HDF P10
STAT-1
DAPI
MERGE
D
% plaques
120
100
80
60
40
20
0
(-)
IFNβ
P1
P3
P5
P10
conditioned media
P10 + nIFNα
P10 + nIFNβ
P1 + DS

In reciprocal experiments, inhibition of IFN activity was found to promote MV replication in otherwise nonsupportive high-passage HDF. Pretreatment of P10 cultures with neutralizing antibodies to human IFN-β allowed MV to spread and form foci (Fig. 6F) and replicate to titers comparable to low-passage cells (Fig. 6H). Consistent with the results of the VSV plaque reduction assays, inhibiting the activity of IFN-α had only modest effects on MV replication in high-passage HDF. Pretreatment with neutralizing antibodies to human IFN-α did not result in foci formation or significant increases in late gene expression (Figs. 6E and G) and did not allow MV to replicate to high titers (Fig. 6H).

Discussion

In the current study, we have demonstrated that MV, a poxvirus commonly reported to be rabbit specific, has the capacity to replicate in primary human fibroblasts in vitro. This finding extends the observations of an earlier report from our laboratory in which MV was also found to productively infect a broad spectrum of human tumor cell lines (Sypula et al., 2004) by demonstrating that IFN responses following MV recognition and entry of primary human cells significantly impact on the outcome of the infection and are critical in determining the cell tropism of the virus. Other recent studies have also indicated that MV tropism in vitro is not restricted to leporine cells, suggesting that the blockade to poxvirus infection in nontraditional host species may be more circumventable than originally suspected. For example, MV has been found to productively infect several simian, murine, feline, and avian cell lines (Comanita and Dekaban, 2004; Johnston et al., 2003; Wang et al., 2004), a phenomenon that also can be linked to the integrity of endogenous IFN responses in these cells. However, it should be noted that MV has never been shown to cause disease in humans or any vertebrate outside the lagomorph family, but it can cause lethal infection in mice deficient for STAT-1 (Wang et al., 2004).

The importance of the IFN family in controlling viral infections is well established (Katze et al., 2002); thus, it is not surprising that the antiviral effects mediated by these cytokines can profoundly influence virus–host interactions. Moreover, the current study indicates that host IFN responses also have the potential to influence the inherent permissiveness of cells from nonhost species to poxvirus infection. MV is predicted to encode immunomodulatory proteins with the potential to target IFN responses mediated by PKR (Barrett et al., 2001; Ramelot et al., 2002), but little is known about the function of these proteins in the context of MV infection let alone their efficacy in cells from nonhost species. However, the results of this study and others (Wang et al., 2004) demonstrating the importance of IFN in permissiveness to MV infection would suggest that the mechanisms employed by MV to counter these innate responses are ineffective in nonpermissive cells. Given the ability of MV to efficiently infect and replicate in rabbit cells, including primary dermal fibroblasts analogous to the human HDF used in the present study, this property is likely species specific. For example, the MV IFN-γ receptor homologue M-T7 is specific for rabbit IFN-γ while the orthologs encoded by the orthopoxviruses have a much broader species specificity (Alcami and Smith, 1996). Because poxviruses typically exhibit a very restrictive host range that has not been attributed to the presence or absence of specific cell surface receptors necessary for virus infection (Esposito and Fenner, 2001), these findings may provide insight into a potential molecular basis for poxvirus host and cell tropism.

Detection of phosphorylated PKR concurrent with phosphorylated eIF-2α indicated that PKR was constitutively activated in high-passage HDFs even in the absence of external stimuli. It is likely that this finding represented the activity of cellular regulators, such as PACT, which are induced by differentiation and stress stimuli and activate PKR leading to transcriptional shutdown (Patel and Sen, 1998; Patel et al., 2000). Yet it is less clear why activation of PKR in high-passage HDF did not correlate with increased apoptosis. High-passage HDFs remain sensitive to the apoptosis induced by dsRNA since both MV infection and treatment with poly(I:C) were associated with increased cytotoxicity. However, we have observed decreased PARP expression in primary HDFs as they are passaged (data not shown), a phenomenon that has also been associated with advanced fibroblast age in other studies (Ly et al., 2000). Thus, it is conceivable that high-passage HDFs are more resistant to the pro-apoptotic effects of sustained PKR activation than low-passage cells in which PARP levels are normal.

The current study also demonstrates the influence of age-related effects on the susceptibility of cultured primary cells to poxvirus infection. Changes in IFN production and sensitivity as fibroblasts age in vitro have been well

Fig. 5. The IFN response pathway is constitutively activated in high-passage HDF. HDFs were cultured for 1–10 passages then seeded at 80% confluence in serum-reduced media. After 24 h, cells were harvested for RNA and protein extraction. Low-passage HDF (P1) stimulated with poly(I:C) dsRNA (DS, 20 μg/ml) served as a control. (A) RT-PCR detection of OAS, PKR, and IFNβ expression. Detection of GAPDH expression (lower panel) ensured equal loading. (B) Western blot detection of unphosphorylated and phosphorylated STAT-1 (Tyr701, Ser727), PKR (Ser31), and eIF-2α (eIF-2α, Ser51). Detection of actin levels in each sample ensured equal loading. (C) Fluorescence microscopy detection of STAT-1α (green) in P1 and P10 HDF. Nuclei are indicated by DAPI counterstain (blue). (D) Detection of relative IFN levels in CM from passaged HDF by VSV plaque reduction assay. Untreated BHK21 cells (−) and BHK21 cells that were preincubated for 6 h with recombinant human IFNβ instead of CM (hIFNβ, 5 U/ml) served as controls. IFN was depleted from CM from P10 cells using neutralizing antibodies directed against IFN-α (nIFNα) or IFN-β (nIFNβ). Cells were stained with crystal violet at 48 h PI to visualize plaques. Values represent mean number of plaques ± SD in triplicate wells expressed as a percentage of plaques in untreated wells.

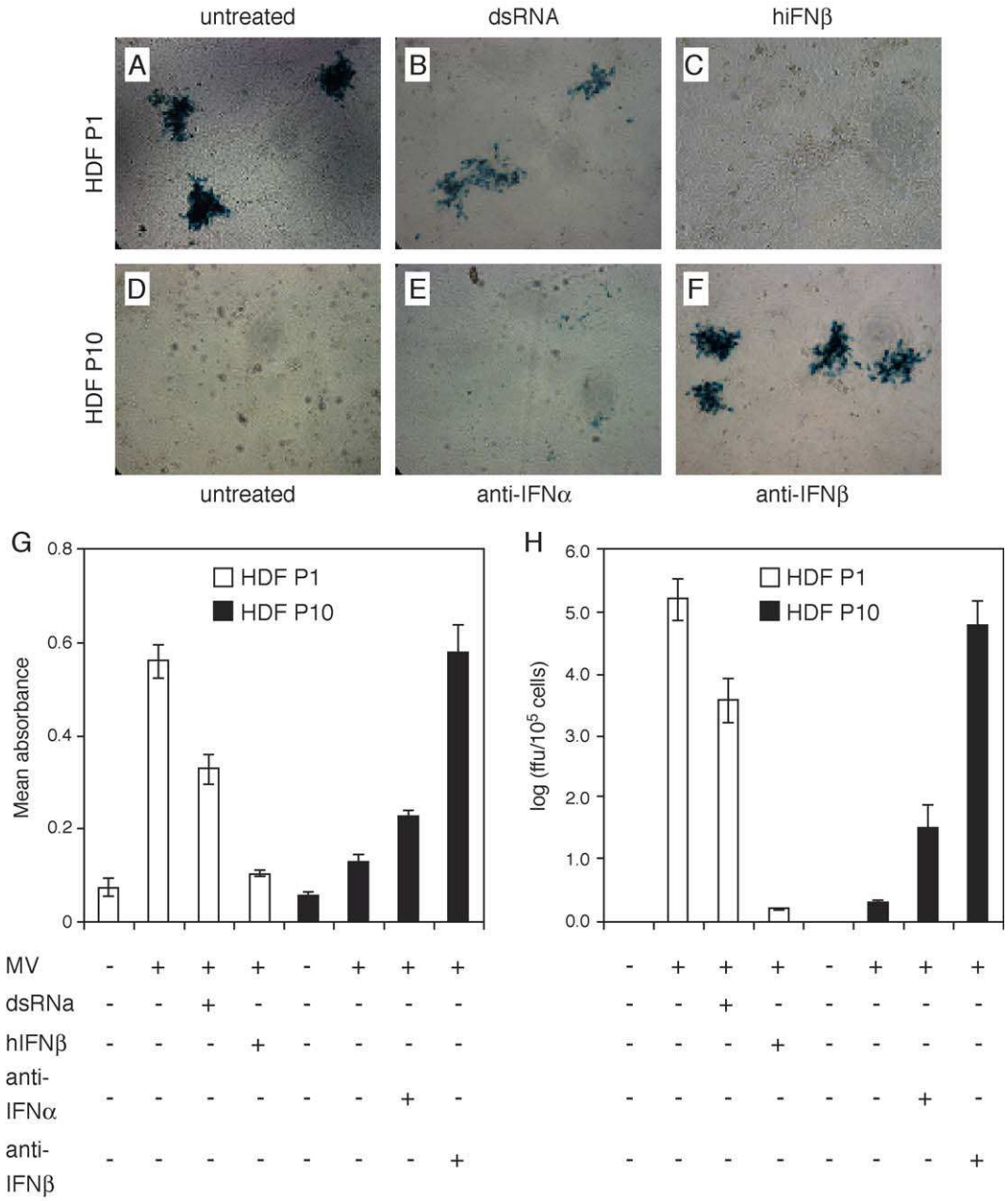

Fig. 6. Manipulation of the IFN response pathway alters the permissiveness of HDF. P1 and P10 HDFs were infected with vMyxlacZ at MOI = 0.1 in the presence or absence of inducers and inhibitors of the IFN response. Infection was assessed by β-galactosidase assay at 48 h PI. (A–C) Infection of P1 HDF in the presence of poly(I:C) dsRNA (B, 20 μg/ml) or recombinant human IFNβ (C, 5 U/ml) decreased MV replication compared to untreated cells (A). (D–F) Pretreatment of P10 HDF with neutralizing antibodies to human IFNβ (F, 100 NU/ml), but not human IFNα (E, 100 NU/ml) rendered cells permissive to MV infection. (G) Quantification of β-galactosidase expression at 48 h PI. Values represent mean absorbance ± SD (corrected for background) from triplicate wells. (H) Viral titers obtained at 48 h PI. Values represent mean focus forming units ± SD from triplicate wells.

characterized for several species (Jordan and Merigan, 1974; Lockart, 1968; Marcus and Carver, 1967; St. Geme and Horrigan, 1969) and shown to involve IFN activity directly at the level of individual cells rather than only reflect the recruitment of more cells within the population to a state of IFN sensitivity (Jordan and Merigan, 1974). Moreover, this property has been associated with changes in susceptibility to infection by viruses known to be exquisitely sensitive to IFN, such as Newcastle disease virus and VSV (Jordan and Merigan, 1974; Lockart, 1968), and for poxviruses such as Vaccinia virus (Gifford et al., 1963; Lindenmann and Gifford, 1963). Since current poxvirus vaccination strategies are contraindicated in those with compromised immune systems, including young children and the elderly (Bennett and Ledell, 2003), further investigation of role of IFN as a determinant of poxvirus tropism may provide insight of use to the development of safer vaccine strategies and the development of novel antiviral agents directed at poxviruses.

IFN sensitivity also forms the basis for therapeutic strategies utilizing viruses, such as the use of VSV as an oncolytic agent (Stojdl et al., 2000). In that regard, poxviruses are being widely investigated as platforms for vaccine development, gene delivery, and oncolytic viral therapies (Essajee and Kaufman, 2004; Guo and Bartlett, 2004; Thorne and Kirn, 2004). In the case of MV, the ability to replicate productively in a majority of human tumor cells tested (Sypula et al., 2004), but not in primary cells that exhibit Type I IFN responses (this manuscript), suggests the potential of MV as an oncolytic virus candidate. This possibility is currently being tested in animal models of human cancers.

Materials and methods

Cells

Primary HDFs were derived from explant cultures of neonatal foreskin tissue as described previously (Vilcek et al., 1978) and grown in Dulbecco's modified Eagle medium (DMEM; GibcoBRL) completed with 10% fetal bovine serum (Sigma), 100 units penicillin/ml, and 100 μg streptomycin/ml. Briefly, foreskin tissue was obtained from healthy neonates of less than 2 weeks of age following elective circumcision conducted according to standard surgical protocols. Tissue was finely minced and individual explants were adhered to culture dishes to stimulate spontaneous cell outgrowth. Explants were cultured for 3 weeks in complete media to allow maximal outgrowth, at which point rapidly replicating HDFs were separated from slowly replicating human epithelial cells (HEP) by low density passaging. Nested RT-PCR detection of fibroblast-specific proline-4-hydroxylase-α (P4Hα) expression in HDF cultures following sustained passaging was used to confirm purity. Purified HDFs were cultured between 1 and 10 passages to achieve the desired level of maturity, amplified to confluence, and stored in liquid nitrogen until used in subsequent experiments. Primary RDFs were prepared in the same manner using dermal tissue obtained from healthy adult New Zealand White rabbits. Baby green monkey kidney (BGMK) cells used to titrate infectious virus and prepare virus stocks were also cultured in complete DMEM.

Viruses and infection

Two derivatives of MV (strain Lausanne) that were created by intergenic insertion of a marker cassette were used for infection studies: vMyxlac, which contains a β-galactosidase cassette driven by a late MV promoter, and vMyxgfp, which contains a green fluorescent protein (GFP) cassette driven by a synthetic Vaccinia virus early/late promoter (Johnston et al., 2003). Both viruses were propagated and titrated by focus formation on BGMK cells as described previously (Opgenorth et al., 1992). For infections, cells were incubated with either virus at the indicated multiplicity of infection (MOI) for 1 h at 37°C, washed to remove excess virus, and cultured in complete media according to experimental parameters. For growth curve studies, cells were initially infected at MOI = 0.1 (multistep) or 5 (single-step) and cultured until harvested. Harvested cells were subjected to three freeze–thaw cycles followed by sonication to release cell-associated virus and viral titers determined as above.

Cytotoxicity assays

High- and low-passage HDFs (2×10^4 cells/well) were seeded in triplicate in 24-well plates and left untreated or subjected to various stress stimuli. Stimuli included infection with vMyxlac at MOI = 0.1 or 5, serum deprivation, and treatment with either the proteasome inhibitor N-Acetyl-Leu-Leu-Norleu-al (LLnL; 10 nM), staurosporine (STS, 50 nM), or poly(I:C) dsRNA (20 μg/ml). Cell viability was assessed at 12 h posttreatment by trypan blue exclusion or Annexin V staining. For trypan blue assays, cells were washed twice with phosphate-buffered saline (PBS), then incubated at room temperature for 15 min in a 0.2% solution of trypan blue dye (Sigma) in PBS. Cells were again washed with PBS and the percentage of viable cells calculated as the number of cells that remained impermeable to the dye divided by the total number of cells. For Annexin V staining, duplicate aliquots of 1×10^5 cells were washed three times in PBS and resuspended in 100 μl of binding buffer (10 mM HEPES-NaOH, 140 mM NaCl, 2.5 mM CaCl2). To each sample, 5 μl of FITC-conjugated Annexin V (Pharmingen) and 2 μl of propidium iodide (PI; Pharmingen) were added followed by incubation at room temperature for 15 min. To control for nonspecific binding, cell aliquots were incubated with Annexin V or PI alone, while cells resuspended in binding buffer alone served as negative controls. Stained cells were immediately analyzed by flow cytometry using FACSCalibur and CellQuest software (Becton Dickson).

β-Galactosidase staining and chromogenic assays

For β-galactosidase expression studies, cells infected with vMyxlac were washed with phosphate-buffered saline (PBS) at various time points postinfection (PI), fixed for 5 min in neutral-buffered formalin (3.7% formaldehyde in PBS), and incubated for 4 h at 37°C with X-gal staining solution (100 μg/ml X-gal, 500 μM potassium ferrocyanide, and 200 μM MgCl2 in PBS). For each experimental condition, the mean number of positive (blue) cells or foci was counted in six high-powered fields from triplicate wells. For chromogenic assays, 3×10^4 cells were seeded in 96-well plates and infected with vMyxlac at the indicated MOI. Infected cells were harvested at various time points PI,

suspended in 150 μl of PBS, and lysed by three freeze–thaw cycles. Fifty microliters of lysate from each sample was transferred to triplicate wells of a 96-well plate and incubated at 37°C for 5 min with 110 μl of reducing buffer (100 mM NaH_2PO_4, 10 mM KCL, 1 mM $MgSO_4$, 50 mM β-mercaptoethanol). Reduced samples were further incubated with 50 μl o-nitrophenyl-β-D-galactopyranoside (ONGP) substrate for 10 min at 37°C and β-galactosidase activity measured by detection of ONGP cleavage at 415 nm using a standard plate reader.

Reverse transcriptase (RT)-PCR analyses

Total cellular RNA was isolated from cultured cells using a RNAeasy Mini Kit (Qiagen) and DNAse treated for 30 min at 37°C. cDNA was prepared using Superscript II RT (Invitrogen) and amplified by 1 cycle (95°C for 1 min), 30 cycles (95°C for 1 min, 55°C for 1 min, 72°C for 2 min), and 1 cycle (72°C for 10 min) with primers specific for each transcript. Primers used included: 5′-acc ttg act gtg tgg aag aaa agc-3′ and 5′-aac aaa gag atg agg ctg ggc g-3′ (PKR), 5′-tgt gtg tgt gtc caa ggt ggt aaa g-3′ and 5′-gaa gtc tct ctg tag ttc tgt gaa gca g-3′ (OAS), 5′-gac agg agg aac ttt gac atc cc-3′ and 5′-act ctg act atg gtc cag gca cag-3′ (IFNβ), and 5′-gat ggg gca ggg gat gtt gac gac-3′ and 5′-gcg gga ggg acg cag cga gac t-3′ (P4Hα). Loading of equal amounts of template cDNA was assessed by amplification of glyceraldehyde-3-phosphate dehydrogenase (GAPDH) at an annealing temperature of 50°C using primers 5′-agc ctt ctc cat ggt ggt gaa gac-3′ and 5′-cgg agt caa cgg att tgg tcg-3′. Amplification of DNAse-treated RNA obtained from each sample prior to reverse transcription served as controls to ensure the lack of contaminating DNA. PCR products were separated by agarose gel electrophoresis and visualized by ethidium bromide staining.

Immunoblot analysis

Cultured cells were lysed in buffer containing 10 mM Tris, pH 4.0, 10 mM NaCl, 3 mM $MgCl_2$, and 0.5% Tween 20, sonicated to solubilize proteins, and cleared by centrifugation. Protein levels were quantified using a protein assay kit (BIO-RAD) and 25 μg of each sample separated by sodium dodecyl sulfate-polyacrylamide gel electrophoresis. Separated proteins were transferred to nitrocellulose and blocked with 5% bovine serum albumin (BSA) in TBST (25 mM Tris-buffered saline, 0.5% Tween 20). Primary antibodies were diluted in 1% BSA-TBST and incubated with membranes for 1 h at room temperature. Membranes were washed and incubated for 1 h at room temperature with horseradish peroxidase-conjugated secondary antibodies diluted 1:3000 in 1% BSA-TBST. Immunoreactive proteins were detected by chemiluminescence (Perkin-Elmer). Loading of equal amounts of protein from each sample was confirmed by detection of the housekeeping gene actin. Mouse monoclonal antibodies specific for actin and STAT-1α were obtained from Santa Cruz Biotechnology Inc, while rabbit polyclonal antibodies specific for STAT-1 phosphorylated at Tyr701 or Ser727 were obtained from Upstate Biotechnology. Rabbit polyclonal antibodies specific for PKR, pPKR (Thr451), eIF-2α, and peIF-2α (Ser51) were obtained from Cell Signaling Technology. Horseradish peroxidase (HRP)-conjugated goat-anti-mouse and goat-anti-rabbit secondary antibodies were obtained from Jackson ImmunoResearch Laboratories Inc.

Immunofluorescence staining and fluorescence microscopy

HDFs were seeded on coverslips coated with poly-L-lysine (Sigma), grown to 80% confluence, and then fixed and permeabilized by incubation with ice-cold methanol for 10 min at 4°C. Fixed cells were washed with PBS and incubated with blocking buffer (10% normal goat serum in PBS) at room temperature for 1 h. Cells were washed with PBS, incubated for 1 h at room temperature with monoclonal antibody specific for human STAT-1α (Santa Cruz Biotechnology Inc) diluted 1:100 dilution in blocking buffer, then washed again in PBS before being incubated for 1 h at room temperature with FITC-conjugated goat-anti-mouse secondary antibody (Jackson ImmunoResearch Laboratories Inc) diluted 1:500 in blocking buffer. After three washes in PBS, cells were counterstained with DAPI reagent (Molecular Probes) for 5 min at 4°C to visualize nuclei. Coverslips were mounted onto glass slides using Prolong Antifade medium (Molecular Probes) to reduce photobleaching and examined by fluorescence microscopy using FITC, brightfield, or DAPI filters. In all immunostaining experiments, isotype control antibodies were used to control for nonspecific antibody binding.

VSV plaque reduction assay

HDF (2×10^5 cells/well) of the indicated passage history were seeded in 12-well plates in serum-reduced medium containing or lacking poly(I:C) dsRNA (20 μg/ml; Sigma). After 24 h, conditioned media (CM) were harvested, cleared by centrifugation, and diluted 1:5 with serum-reduced medium. Subconfluent BHK21 cells were preincubated for 6 h at 37°C with human IFNβ (5 U/ml; BioSource International Inc) or 1 ml of the diluted CM, washed once with PBS, then infected with 25 pfu of vesicular stomatitis virus (VSV). VSV was adsorbed for 1 h at 37°C, at which point the inoculum was removed and cells overlayed with a 60:40 mixture of DMEM and 1% agarose. Infected cells were incubated at 37°C for 48 h and plaques were visualized by crystal violet staining (0.07% crystal violet and 5.5% formaldehyde in PBS). To confirm that IFN was responsible for any reduction in plaque formation observed, CM from P10 HDF was pretreated with 100 NU/ml of neutralizing antibodies against either human IFN-α or IFN-β (BioSource International Inc).

Acknowledgments

G.M. holds a Canada Research Chair in Molecular Virology. J.B.J. is a Canadian Institutes of Health Research (CIHR) Fellow. We thank the pediatric staff of St. Joseph's Hospital, London, ON, Canada, for assistance in acquiring primary tissues. This work was supported by a CIHR operating grant.

References

Alcami, A., Smith, G.L., 1996. Soluble interferon-gamma receptors encoded by poxviruses. Comp. Immunol. Microbiol. Infect. Dis. 19 (4), 305–317.

Barnes, B., Lubyova, B., Pitha, P.M., 2002. On the role of IRF in host defense. J. Interferon Cytokine Res. 22 (1), 59–71.

Barrett, J.W., Cao, J.X., Hota-Mitchell, S., McFadden, G., 2001. Immunomodulatory proteins of myxoma virus. Semin. Immunol. 13 (1), 73–84.

Bennett, M.E., Ledell, K., 2003. Current infection-control issues for smallpox disease and vaccinia vaccine. J. Lab. Clin. Med. 142 (4), 239–245.

Camus-Bouclainville, C., Fiette, L., Bouchiha, S., Pignolet, B., Counor, D., Filipe, C., Gelfi, J., Messud-Petit, F., 2004. A virulence factor of myxoma virus colocalizes with NF-kappaB in the nucleus and interferes with inflammation. J. Virol. 78 (5), 2510–2516.

Comanita, L., Dekaban, G., 2004. Personal communication.

Esposito, J.J., Fenner, F., 2001. Poxviruses, 4th ed. In: Knipe, D.M., Howley, P.M. (Eds.), Fields Virol., vol. 2. Lippincott Williams and Wilkins, Philadelphia, pp. 2885–2921. 2 vols.

Essajee, S., Kaufman, H.L., 2004. Poxvirus vaccines for cancer and HIV therapy. Expert. Opin. Biol. Ther. 4 (4), 575–588.

Fenner, F., Ratcliffe, F., 1965. Myxomatosis. Cambridge Univ. Press, Cambridge, UK.

Gifford, G.E., Toy, S.T., Lindenmann, J., 1963. Studies on vaccinia virus plaque formation and its inhibition by interferon: II. Dynamics of plaque formation by vaccinia virus in the presence of interferon. Virology 19, 294–301.

Greber, U.F., 2002. Signalling in viral entry. Cell. Mol. Life Sci. 59 (4), 608–626.

Guo, Z.S., Bartlett, D.L., 2004. Vaccinia as a vector for gene delivery. Expert Opin. Biol. Ther. 4 (6), 901–917.

Johnston, J.B., Barrett, J.W., Chang, W., Chung, C.S., Zeng, W., Masters, J., Mann, M., Wang, F., Cao, J., McFadden, G., 2003. Role of the serine-threonine kinase PAK-1 in myxoma virus replication. J. Virol. 77 (10), 5877–5888.

Jordan, G.W., Merigan, T.C., 1974. Quantitative aspects of interferon-induced plaque reduction: effects of cell age and dose of challenge virus. Proc. Soc. Exp. Biol. Med. 145 (3), 1037–1041.

Julkunen, I., Linnavuori, K., Hovi, T., 1982. Sensitive interferon assay based on immunoenzymatic quantification of viral antigen synthesis. J. Virol. Methods 5 (2), 85–91.

Katze, M.G., He, Y., Gale Jr., M., 2002. Viruses and interferon: a fight for supremacy. Nat. Rev., Immunol. 2 (9), 675–687.

Kerr, P., McFadden, G., 2002. Immune responses to myxoma virus. Viral Immunol. 15 (2), 229–246.

Komatsu, H., Maehara, N., Shimoda, K., Mori, T., Lee, T., Makino, S., Matumoto, M., 1981. Production of interferon in human diploid cells at different population doubling levels. Arch. Virol. 70 (4), 367–371.

Lalani, A.S., Masters, J., Zeng, W., Barrett, J., Pannu, R., Everett, H., Arendt, C.W., McFadden, G., 1999. Use of chemokine receptors by poxviruses. Science 286 (5446), 1968–1971.

Lau, J.F., Horvath, C.M., 2002. Mechanisms of type I interferon cell signaling and STAT-mediated transcriptional responses. Mt. Sinai J. Med. 69 (3), 156–168.

Levy, D.E., Marie, I., Prakash, A., 2003. Ringing the interferon alarm: differential regulation of gene expression at the interface between innate and adaptive immunity. Curr. Opin. Immunol. 15 (1), 52–58.

Lindenmann, J., Gifford, G.E., 1963. Studies on vaccinia virus plaque formation and its inhibition by interferon: III. A simplified plaque inhibition assay of interferon. Virology 19, 302–309.

Lockart, R.Z., 1968. In: Sanders, M., Lennette, E.H. (Eds.), Medical and Applied Virology. Warren H. Green Inc., St. Louis, pp. 45.

Ly, D.H., Lockhart, D.J., Lerner, R.A., Schultz, P.G., 2000. Mitotic misregulation and human aging. Science 287 (5462), 2482–2486.

Malmgaard, L., 2004. Induction and regulation of IFNs during viral infections. J. Interferon Cytokine Res. 24 (8), 439–454.

Marcus, P.I., Carver, D.H., 1967. Intrinsic interference: a new type of viral interference. J. Virol. 1 (2), 334–343.

Masters, J., Hinek, A.A., Uddin, S., Platanias, L.C., Zeng, W., McFadden, G., Fish, E.N., 2001. Poxvirus infection rapidly activates tyrosine kinase signal transduction. J. Biol. Chem. 276 (51), 48371–48375.

Mims, C.A., 1989. The pathogenetic basis of viral tropism. Am. J. Pathol. 135 (3), 447–455.

Moss, B., 2001. Poxviridae: the virus and their replication. 4 ed. In: Knipe, D.M., Howley, P.M. (Eds.), Fields Virol., vol. 2. Lippincott Williams and Wilkins, Philadelphia, pp. 2849–2883. 2 vols.

Opgenorth, A., Graham, K., Nation, N., Strayer, D., McFadden, G., 1992. Deletion analysis of two tandemly arranged virulence genes in myxoma virus, M11L and myxoma growth factor. J. Virol. 66 (8), 4720–4731.

Patel, R.C., Sen, G.C., 1998. PACT, a protein activator of the interferon-induced protein kinase, PKR. EMBO J. 17, 4379–4390.

Patel, C.V., Handy, I., Goldsmith, T., Patel, R.C., 2000. PACT, a stress-modulated cellular activator of interferon-induced doubles-stranded RNA-activated protein-kinase, PKR. J. Biol. Chem. 275 (48), 37993–37998.

Ramelot, T.A., Cort, J.R., Yee, A.A., Liu, F., Goshe, M.B., Edwards, A.M., Smith, R.D., Arrowsmith, C.H., Dever, T.E., Kennedy, M.A., 2002. Myxoma virus immunomodulatory protein M156R is a structural mimic of eukaryotic translation initiation factor eIF2alpha. J. Mol. Biol. 322 (5), 943–954.

Schneider-Schaulies, J., 2000. Cellular receptors for viruses: links to tropism and pathogenesis. J. Gen. Virol. 81 (Pt. 6), 1413–1429.

Seet, B.T., Johnston, J.B., Brunetti, C.R., Barrett, J.W., Everett, H., Cameron, C., Sypula, J., Nazarian, S.H., Lucas, A., McFadden, G., 2003. Poxviruses and immune evasion. Annu. Rev. Immunol. 21, 377–423.

Servant, M.J., Grandvaux, N., Hiscott, J., 2002. Multiple signaling pathways leading to the activation of interferon regulatory factor 3. Biochem. Pharmacol. 64 (5–6), 985–992.

St. Geme Jr., J.W., Horrigan, D.S., 1969. Comparative production of interferon by foreskin fibroblasts from newborn infants and children. J. Lab. Clin. Med. 74 (6), 946–949.

Stojdl, D.F., Lichty, B., Knowles, S., Marius, R., Atkins, H., Sonenberg, N., Bell, J.C., 2000. Exploiting tumor-specific defects in the interferon pathway with a previously unknown oncolytic virus. Nat. Med. 6 (7), 821–825.

Sypula, J., Wang, F., Ma, Y., Bell, J., McFadden, G., 2004. Myxoma virus tropism in human tumor cells. Gene Ther. Mol. Biol. 8, 103–114.

Tamura, M., Sasakawa, S., 1983. Induction of human leukocyte interferon by heat-treated poly I: poly C. Biochem. Biophys. Res. Commun. 110 (3), 851–858.

Taniguchi, T., Takaoka, A., 2002. The interferon-alpha/beta system in antiviral responses: a multimodal machinery of gene regulation by the IRF family of transcription factors. Curr. Opin. Immunol. 14 (1), 111–116.

Thorne, S.H., Kirn, D.H., 2004. Future directions for the field of oncolytic virotherapy: a perspective on the use of vaccinia virus. Expert Opin. Biol. Ther. 4 (8), 1307–1321.

Vilcek, J., Havell, E.A., Gradoville, M.L., Mika-Johnson, M., Douglas, W.H., 1978. Selection of new human foreskin fibroblast cell strains for interferon production. Adv. Exp. Med. Biol. 110, 101–118.

Wang, F., Ma, Y., Barrett, J., Gao, X., Loh, J., Barton, E., Virgin IV, H.W., McFadden, G., 2004. Disruption of ERK1/2 MAP kinase-dependent induction of type I interferon breaks myxoma virus species barrier. Nat. Immunol. 5, 1266–1274.

Williams, B.R., Sen, G.C., 2003. Immunology. A viral on/off switch for interferon. Science 300 (5622), 1100–1101.